NATIONAL ADVISORY COMMITTEE FOR AERONAUTICS

TECHNICAL NOTE 3907

SIMILITUDE RELATIONS FOR FREE-MODEL WIND-TUNNEL STUDIES OF STORE-DROPPING PROBLEMS

By Carl A. Sandahl and Maxime A. Faget

Langley Aeronautical Laboratory
Langley Field, Va.



Washington January 1957 L

TECHNICAL NOTE 3907

SIMILITUDE RELATIONS FOR FREE-MODEL WIND-TUNNEL

STUDIES OF STORE-DROPPING PROBLEMS

By Carl A. Sandahl and Maxime A. Faget

SUMMARY

Two methods are presented for dynamically scaling store models for wind-tunnel store-dropping studies. For each method the model and prototype Mach numbers are assumed to be necessarily equal and the Reynolds number effects are assumed to be negligible. The light-model method gives exact simulation of the store motions except that the vertical displacements are deficient. This deficiency is reduced as the vertical ejection velocity is increased or it can be eliminated by accelerating the parent model upward at the instant of store separation. The heavy-model method, in which the parent model is stationary, gives complete simulation of the store motion except that the short-period longitudinal oscillation is too poorly damped; this defect is of no serious consequence during the first phase of a drop because the time during which the store is critically close to the parent model is generally small compared with the period of the longitudinal oscillation. The heavy-model method is generally recommended for store-dropping studies; however, it is often impossible to make the models sufficiently heavy and with the proper moment of inertia. If such is the case, the light-model method is required.

A brief description of the method of conducting store-dropping tests in the preflight jet of the Langley Pilotless Aircraft Research Station at Wallops Island, Va., is given.

INTRODUCTION

Investigators have, for some time, been using the free-model technique in wind tunnels to study the motions of stores and missiles during and following release from a parent airplane. In this method, a model of all or part of the parent airplane is placed in the tunnel test section and the store or missile model is dropped or propelled into the airstream. The unrestrained dynamic behavior of the store or missile model in the presence of the interference field is recorded by means of high-speed photography.

In making tests in the aforementioned manner, it is necessary, of course, to scale the models in a manner which will determine the relations between the translational and rotational motions of the model and the prototype. The general subject of scaling aerodynamic models for free-flight testing has been thoroughly discussed in references 1 and 2. In the present report, the scaling relations have been derived in a manner which permits an insight into the specific problems of free-model drop testing in wind tunnels. Some of the deficiencies of the test method are noted and methods by which the initial conditions may be adjusted to circumvent these deficiencies are presented. In addition, a brief description of the free-flight drop-model technique as employed in the preflight jet of the Langley Pilotless Aircraft Research Station at Wallops Island, Va., is given in the appendix.

SYMBOLS

linear horizontal displacement Х aerodynamic force coefficient in horizontal plane $C_{\mathbf{x}}$ ratio of specific heats Y static pressure p Mach number M $K_S = \frac{S}{T.2}$ reference area S characteristic length L number of characteristic lengths N average model weight density Б acceleration due to gravity g $K_V = \frac{V}{T^3}$ volume

$$K_{X} = \frac{C_{X} \frac{\gamma}{2} M^{2} K_{S}}{K_{V}}$$

t time

z linear vertical displacement

$$K_{z} = \frac{C_{z} \frac{\gamma}{2} M^{2} K_{S}}{K_{V}}$$

C_Z aerodynamic force coefficient in vertical plane

tx time required to move a specified number of characteristic lengths in horizontal plane

θ pitch angle

C_θ total aerodynamic moment coefficient

 $K_R = \frac{k}{L}$

k radius of gyration

 $K_{\theta} = \frac{C_{\theta} \frac{\gamma}{2} M^2 K_{S}}{K_{V} K_{R}^2}$

 $\alpha_{z,tx}^{\bullet}$ angle of attack contributed by \dot{z} at $t = t_{x}$

U stream velocity

P period of oscillation

 $c_{m_{\alpha}}$ static pitching-moment derivative

t_{1/2} time to damp oscillation

W weight

q dynamic pressure

 $\left(C_{m_{\theta}^{\bullet}} + C_{m_{\alpha}^{\bullet}}\right)$ total damping derivative

C_{L_a} lift-curve slope

T stream static temperature

 K_{ax} specified horizontal load factor

K_{az} specified vertical load factor

Subscripts:

0 condition at $t_x = 0$

M model

P prototype

Dots over quantities indicate derivatives with respect to time. The coordinate system is illustrated in figure 1.

MODEL-SCALING EQUATIONS

General

In making free-model tests, it is necessary to scale the model dimensions, weight, and inertia in a manner which will determine the relations between the translational and the rotational motions of the model and the prototype. The primary requirement is that the trajectories of the model and prototype be as nearly geometrically similar as possible. The method of analysis consists of writing expressions for the translational and rotational motions and for the period and damping of the shortperiod longitudinal oscillation. Examination of these equations indicates those parameters required for the particular simulation desired. basic methods of simulation are described; in each, it is assumed that the model and prototype Mach numbers are equal and that Reynolds number effects are negligible. In the first method, the aerodynamically produced translational accelerations vary inversely with the characteristic length; this method is best suited for dynamic stability studies and for store-dropping studies where a large vertical ejection velocity is used. In the second method, the aerodynamically produced accelerations are independent of characteristic length just as are the gravity-produced accelerations; this method is required for free-dropping store studies. The first and second simulation methods will be called the light-model method and the heavymodel method, respectively, for the purposes of the present report.

The present method of analysis may appear more tedious than the classical dimensional analysis given, for example, in reference 3. Both methods yield the same dimensional relations between the model and the

prototype. However, the present method shows how some of the deficiencies inherent in the model tests may be circumvented by adjusting the initial conditions.

Light-Model Method

The equations for linear motions in the horizontal plane are

$$\ddot{x} = \frac{C_x \frac{\gamma}{2} p M^2 K_S L^2 g}{dK_V L^3} = \frac{K_x pg}{dL}$$
 (1)

$$\dot{x} = \dot{x}_0 + \frac{K_X pg}{dL} t \tag{2}$$

$$x = \dot{x}_0 t + \frac{K_x pg}{2dL} t^2$$
 (3)

where \dot{x}_0 is the horizontal velocity at t=0 and K_x contains those quantities which are assumed to be independent of L. The quantity $\frac{K_x p}{dL}$ is the ratio of aerodynamic force to weight (load factor); if $\frac{p}{d}$ is constant, the load factor and, consequently, \ddot{x} are inversely proportional to L.

An expression for the time t_X required to move a specified number of characteristic lengths NL in the horizontal plane is required. From equation (3) with $\dot{\mathbf{x}}_0$ = 0 and x = NL, the following is true:

$$t_{x} = \sqrt{\frac{2dNL^{2}}{K_{x}pg}}$$
 (4)

Therefore, t_x is proportional to L if $\frac{p}{d}$ is constant. Substituting t_x (from eq. (4)) for t in equations (2) and (3) shows that \dot{x}_{tx} and x_{tx} (conditions when $t=t_x$) are independent of and proportional to L, respectively.

The equations for linear motions in the vertical plane are

$$\ddot{z} = \left(1 + \frac{K_Z p}{dL}\right) g \tag{5}$$

$$\dot{z} = \dot{z}_{O} + \left(1 + \frac{K_{Z}p}{dL}\right)gt \tag{6}$$

$$z = \dot{z}_{O}t + \left(1 + \frac{K_{z}p}{dL}\right)\frac{gt^{2}}{2}$$
 (7)

where $\frac{K_z p}{dL}$ is the vertical load factor.

Substituting t_X (from eq. (4)) for t in equations (6) and (7) shows that \dot{z} and z approach independence of and proportionality to L, respectively, only as the vertical load factor or \dot{z}_0 becomes large. Consequently, the vertical and horizontal motions do not scale identically for the conditions so far established. The vertical launching velocity may, however, be adjusted so that the ratio of vertical to horizontal displacement at a specified value of t_X will be equal for model and prototype. Substituting t_X (from eq. (4)) for t in equation (7) and dividing by x = NL yields

$$\left(\frac{z}{x}\right)_{t_{x}} = \frac{1 + \frac{K_{z}p}{dL}}{\frac{K_{x}p}{dL}} + \frac{\dot{z}_{0}}{\sqrt{\frac{K_{x}pgN}{2d}}}$$
(8)

It is desired that this ratio be equal for model and prototype when $t=t_{\mathbf{x}}$ as defined by equation (4). Writing equation (8) for model and prototype gives

$$\dot{z}_{O,M} = \dot{z}_{O,P} + \sqrt{\frac{gdN}{2K_{x}p}} (L_{P} - L_{M})$$
 (9)

where subscript M denotes model and subscript P denotes prototype.

This value of $\dot{z}_{0,M}$ will make $\left(\frac{z}{x}\right)_{t_X}$ equal for model and prototype. For a typical case where $\frac{K_x p}{d}$ is such as to give a load factor of 20 for a $\frac{1}{20}$ - scale model with characteristic length equal to 0.5 foot and N = 1,

$$\dot{z}_{O,M} = \dot{z}_{O,P} + \sqrt{\frac{(32.2)(1)}{(2)(10)}} (10 - 0.5)$$

= $\dot{z}_{O,P} + 12.1$ ft/sec

Some prototype trajectories and model trajectories, adjusted in the above manner, are compared in figure 2. The agreement is improved as \dot{z}_0 is increased. It should be noted that adjusting $\dot{z}_{0,M}$ in the aforementioned manner results in slightly different trajectories and time-distance histories for model and prototype. Consequently, the interference field will affect the model and prototype differently. This difference is believed to be negligible in most cases.

The equations for the rotational motions are

$$\dot{\theta} = \dot{\theta}_{0} + \frac{K_{\theta}pg}{dL^{2}} t \tag{11}$$

$$\theta = \dot{\theta}_0 t + \frac{K_0 pg}{2dL^2} t^2 \tag{12}$$

The rotational accelerations vary inversely with L^2 rather than with L as was the case for the linear accelerations. Substituting $t_{\rm X}$ (from eq. (4)) for t in equation (12) gives

$$\theta_{\text{tx}} = L\dot{\theta}_{\text{O}} \sqrt{\frac{2dN}{K_{x}pg}} + \frac{K_{\theta}N}{K_{x}}$$
 (13)

Therefore, θ_{tx} is independent of L provided that $L\dot{\theta}_0$ and $\frac{d}{p}$ are constant. The same substitution into equation (11) along with the condition that $L\dot{\theta}_0$ = Constant gives

$$\dot{\theta}_{tx} = \frac{\text{Constant}}{L} + \frac{K_{\theta}}{L} \sqrt{\frac{2pNg}{dK_X}}$$
 (14)

Therefore, $\dot{\theta}_{tx}$ is inversely proportional to L.

Equation (13) establishes that θ_{tx} is independent of L; therefore, the contribution of θ_{tx} to the angle of attack at $t=t_x$ is correct. However, in model tests, \dot{z} at $t=t_x$ is always too small because the contribution due to gravity is too small, even when the condition for $\dot{z}_{0,M}$ (eq. (9)) is imposed. Consequently, the contribution of \dot{z} to the angle of attack at $t=t_x$ is too small. The angle of attack due to \dot{z} at $t=t_x$, $\alpha_{\dot{z},tx}$, is approximated by the ratio of \dot{z}_{tx} to the horizontal velocity of the model relative to the air. Writing this ratio by means of equations (2) and (6) with the substitution of t_x (from eq. (4)) for t gives

$$\alpha_{z,tx}^{\bullet} = \frac{\dot{z}_{0} + \left(1 + \frac{K_{z}p}{dL}\right)\sqrt{\frac{2gdNL^{2}}{K_{x}p}}}{U - \sqrt{\frac{2K_{x}pgN}{d}}}$$
(15)

Writing equation (15) for model and prototype conditions, subtracting, and inserting the condition for $\dot{z}_{0,M}$ (from eq. (9)) gives the following for the error in the angle of attack at $t=t_x$:

$$\left(\alpha_{z,tx}^{\bullet}\right)_{M} - \left(\alpha_{z,tx}^{\bullet}\right)_{P} = \Delta\alpha_{tx} = \frac{\sqrt{\frac{gND}{2K_{x}p}}\left(I_{M} - I_{P}\right)}{U - \sqrt{\frac{2gNK_{x}p}{d}}}$$
(16)

L

As an example, using the same model values as for the example following equation (9), and setting U equal to 2,000 feet per second gives for equation (16)

$$\Delta \alpha_{\text{tx}} = \frac{\sqrt{\frac{(32.2)(1)}{(2)(10)}}(0.5 - 10)}{2000 - \sqrt{(2)(32.2)(1)(10)}}$$
$$= -0.0061 \text{ radian or } -0.35^{\circ}$$

If the condition $\dot{z}_{0,M}=\dot{z}_{0,P}$ is used instead of equation (9), the error will be just twice as large as that given by equation (16). In model tests where this method of simulation is employed, the angle of attack at $t=t_x$ is always too small by an amount given by equation (16). Should particular conditions warrant, $\alpha_{0,M}$ could be increased by an amount equal to $\Delta\alpha_{tx}$.

The period of the short-period longitudinal oscillation, P, is well approximated by

$$P = 2\pi \sqrt{\frac{dK_V L^3 K_R^2 L^2}{C_{m_{\alpha}} \frac{\gamma}{2} pM^2 K_S L^2 L}}$$

$$= (Constant) L \sqrt{\frac{d}{p}}$$
(17)

The period is proportional to L provided that $\frac{d}{p}$ is constant.

The time to damp the short-period oscillation may be written as

$$t_{1/2} = \frac{WU}{gqS} \left[\frac{0.693}{\left(\frac{C_{m\dot{\theta}} + C_{m\dot{\alpha}} \right) \left(\frac{L}{k} \right)^{2}}{2} - C_{L_{\alpha}} \right]$$

$$= \frac{K_{V}L^{3}dM}{g} \sqrt{\gamma kT} \left[\frac{0.693}{\left(\frac{C_{m\dot{\theta}} + C_{m\dot{\alpha}} \right) \left(\frac{L}{k} \right)^{2}}{2} - C_{L_{\alpha}} \right]$$

$$= (Constant) \frac{d}{p} \sqrt{T}L$$
(18)

10 NACA TN 3907

The time to damp is proportional to L provided that $\frac{d}{p}$, $\frac{L}{k}$, and T are constant.

The conditions and results for the foregoing light-model simulation are summarized in table I.

The condition that $\frac{p}{d}$ is constant results in the following equations for the model and prototype.

$$W_{M} = W_{P} \frac{p_{M}}{p_{P}} \left(\frac{I_{M}}{I_{P}} \right)^{3}$$
 (19)

$$d_{M} = d_{P} \left(\frac{p_{M}}{p_{P}} \right) \tag{20}$$

Modified Light-Model Method

As pointed out earlier, the gravity component of the vertical acceleration is deficient in model tests utilizing the light-model simulation. One method of circumventing this problem is to accelerate the parent model upward at a value equal to $\left(\frac{L_p}{I_M}-1\right)g$. A photograph of a test setup utilizing this idea is shown in figure 3. The parent model is mounted so as to have vertical freedom only; the acceleration in this case is produced by a combination of wing lift and a pneumatic cylinder. With this arrangement, the trajectory of the store relative to the parent model may be made to duplicate exactly the prototype trajectory. Equations (1) to (4) and (10) to (20) apply without modification; equations (5) to (9) are inconsequential because the trajectories are correct without adjusting $\frac{L_p}{L_p}$. The modified light-model simulation is summarized in table I.

Heavy-Model Method

In this method, the aerodynamically produced accelerations are forced to be independent of L. The equations of linear horizontal motions are

$$\ddot{x} = \frac{K_{x}pg}{dL} = K_{ax}g \tag{21}$$

$$\dot{x} = \dot{x}_0 + K_{ax}gt \tag{22}$$

$$x = \dot{x}_0 t + \frac{1}{2} K_{ax} g t^2$$
 (23)

where the value of K_{ax} is the value of the horizontal load factor which is held constant during scaling.

From equation (21)

$$\frac{\mathbf{p}}{\mathbf{d}} = \frac{K_{\mathbf{a}\mathbf{x}}^{\mathbf{L}}}{K_{\mathbf{x}}} \tag{24}$$

In this method $\frac{p}{d}$ is proportional to L. The substitution for $\frac{p}{d}$ from equation (24) will now be made for the equations in the previous sections of this report.

Solving equation (23) with $\dot{x}_0 = 0$ and x = NL gives

$$t_{x} = \sqrt{\frac{2NL}{K_{ax}g}}$$
 (25)

From equations (22) and (23), \dot{x}_{tx} and x_{tx} are proportional to \sqrt{L} and L, respectively, provided that $\dot{x}_0 = 0$.

The equations for vertical linear motions are

$$\ddot{z} = \left(1 + \frac{K_z p}{dL}\right) g = \left(1 + K_{az}\right) g \tag{26}$$

$$\dot{z} = \dot{z}_0 + \left(1 + K_{az}\right) gt \tag{27}$$

$$z = \dot{z}_0 t + \frac{1}{2} (1 + K_{az}) g t^2$$
 (28)

where the value of K_{ax} is the value of the vertical load factor which is held constant during scaling.

Comparison of equations (21) to (23) with equations (26) to (28) shows that the vertical and horizontal motions scale identically provided that $\dot{\mathbf{x}}_0 = \dot{\mathbf{z}}_0 = 0$. Consequently, the trajectories, normalized with respect to L, will be identical. However, for the case where $\dot{\mathbf{x}}_0 = 0$ and $\dot{\mathbf{z}}_0 \neq 0$, this is not true and it will be necessary to adjust $\dot{\mathbf{z}}_{0,M}$ to make $\left(\frac{\mathbf{z}}{\mathbf{x}}\right)_{t_X}$ equal for model and prototype. Substituting t_X (eq. (25)) into equation (28) and dividing by $\mathbf{x} = NL$ gives

$$\left(\frac{z}{x}\right)_{t_{X}} = \dot{z}_{0} \sqrt{\frac{2}{K_{ax}gNL}} + \frac{1 + K_{az}}{K_{ax}}$$
 (29)

Writing this equation for model and prototype, equating, and solving for $\dot{z}_{\text{O.M}}$ gives

$$\dot{z}_{O,M} = \dot{z}_{O,P} \sqrt{\frac{L_{M}}{L_{P}}}$$
 (30)

In the heavy-model simulation, $\dot{z}_{0,M}$ is less than $\dot{z}_{0,P}$; whereas, in the light-model simulation, the reverse is true. An example of the heavy-model simulation is given in figure 4.

Placing the restriction of equation (30) on equations (27) and (28) and substituting t_x for t shows that \dot{z}_{tx} is proportional to \sqrt{L} and z_{tx} is proportional to L_{\bullet}

The equations for rotational motions are obtained by substituting for $\frac{p}{d}$ from equation (24) in equations (10), (11), and (12).

$$\ddot{\theta} = \frac{K_{\theta}K_{ax}g}{K_{x}L} \tag{31}$$

$$\dot{\theta} = \dot{\theta}_0 + \frac{K_\theta K_{ax} g}{K_x L} t$$
 (32)

$$\theta = \dot{\theta}_0 t + \frac{1}{2} \frac{K_0 K_{ax} g}{K_x L} t^2$$
 (33)

Substituting t_x (from eq. (25)) for t gives

$$\theta_{\text{tx}} = \dot{\theta}_{\text{O}} \sqrt{\frac{2\text{NL}}{K_{\text{ax}}g}} + \frac{K_{\theta}N}{K_{\text{x}}}$$
 (34)

Therefore, $\theta_{\rm tx}$ is independent of L provided that $\sqrt{L\dot{\theta}_0}$ is constant. With the substitution for t and the condition that $\sqrt{L\dot{\theta}_0}$ = Constant, equation (32) gives

$$\dot{\theta}_{\text{tx}} = \frac{\text{Constant}}{\sqrt{L}} + \frac{K_{\theta}}{K_{x}} \sqrt{\frac{2NK_{ax}g}{L}}$$
 (35)

Since θ_{tx} is independent of L, its contribution to α_{tx} is correct; however, because \dot{z}_{tx} is proportional to \sqrt{L} , the contribution of \dot{z}_{tx} to α_{tx} is too small. Following the development for equation (15) and using equations (22), (25), and (27) gives

$$\alpha_{z,tx}^{\cdot} = \frac{\dot{z}_{0} + (1 + K_{az})g\sqrt{\frac{2NL}{K_{ax}g}}}{U - K_{ax}g\sqrt{\frac{2NL}{K_{ax}g}}}$$
(36)

Writing for model and prototype and including condition for $\dot{z}_{\rm tx}$ (from eq. (30)), gives

$$\Delta \alpha_{\text{tx}} = \left(\alpha_{\text{z},\text{tx}}^{\bullet}\right)_{\text{M}} - \left(\alpha_{\text{z},\text{tx}}^{\bullet}\right)_{\text{P}}$$

$$= \frac{\dot{z}_{\text{O,M}} \left(1 - \sqrt{\frac{\text{Lp}}{\text{I}_{\text{M}}}}\right) + \left(1 + K_{\text{az}}\right) \sqrt{\frac{2g}{K_{\text{ax}}}} \left(\sqrt{(\text{NL})_{\text{M}}} - \sqrt{(\text{NL})_{\text{p}}}\right)}$$
(37)

If the condition $\dot{z}_{0,M} = \dot{z}_{0,P}$ is used instead of equation (30), the correction is given by equation (37) except that $\dot{z}_{0,M} \left(1 - \sqrt{\frac{L_P}{L_M}}\right) = 0$. Substituting some typical values gives

$$\Delta \alpha_{\text{tx}} = \frac{(20) \left(1 - \sqrt{20}\right) + (1 + 0.5) \sqrt{\frac{(2)(32.2)}{2}} \left(\sqrt{0.5} - \sqrt{10}\right)}{2000}$$

$$= -0.0452 \text{ radian or } -2.6^{\circ}$$

This error may be appreciable, and whether it may be desired to adjust $\alpha_{0,M}$ will depend on the particular testing situation. The error is larger for the heavy-model simulation than for the light-model simulation because \dot{z}_{tx} is approximately proportional to \sqrt{L} for the former and approximately independent of L for the latter.

The period P obtained from equation (17) by imposing the condition of equation (24) is

$$P = (Constant) \sqrt{L}$$
 (38)

The period is properly scaled.

The time to damp obtained from equation (18) and equation (24) is

$$t_{1/2} = (Constant) \sqrt{T}$$
 (39)

The models will therefore be too lightly damped.

The heavy-model simulation is summarized in table I. The condition that $\frac{p}{d} = \frac{K_{ax}L}{K_{x}}$ gives

$$d_{M} = \frac{L_{P}}{L_{M}} \frac{p_{M}}{p_{P}} d_{P} \tag{40}$$

$$W_{M} = \left(\frac{I_{M}}{I_{P}}\right)^{2} \frac{p_{M}}{p_{P}} W_{P} \tag{41}$$

CONCLUDING REMARKS

Two methods, the light model and the heavy model, have been presented for dynamically scaling store models for wind-tunnel store-dropping studies. In each, it is assumed that the model and prototype Mach numbers are necessarily equal and that Reynolds number effects are negligible. The light-model method gives exact simulation for all the motions except that the gravity component of the vertical acceleration and, consequently, the vertical displacement between the store model and the parent airplane model is deficient. The effect of this deficiency on the trajectory is reduced as the vertical ejection velocity is increased. This deficiency is eliminated completely by a modification of the light-model method, wherein the parent model is accelerated upward at a rate which offsets the gravity deficiency. This modified light-model method provides complete simulation of the store motion for any ejection velocity. Either of the light-model simulation methods will simulate accurately the oscillatory characteristics of the store. The basic light-model method may be used when the ejection velocities are large; the modified method should be used when the ejection velocity approaches zero.

The heavy-model method simulates exactly the trajectory of the store when the parent model is stationary; the need for accelerating the parent model as in the modified light-model method is obviated. The heavy-model method gives exact simulation of all the store motions except that the short-period longitudinal oscillation is too poorly damped; this defect is inconsequential because the time during which the store model is critically close to the parent model is generally small compared with the period of the longitudinal oscillation of the store. Thus, when simulation may be achieved by the heavy-model method, it is recommended. Experience has shown, however, that it is often impossible to make the models sufficiently heavy and with the proper moment of inertia to satisfy the heavy-model method, particularly when simulating high altitude drops in a sea-level facility such as the preflight jet of the Langley Pilotless Aircraft Research Station at Wallops Island, Va. Store construction problems may, in fact, dictate the method of simulation.

Langley Aeronautical Laboratory,
National Advisory Committee for Aeronautics,
Langley Field, Va., October 3, 1956.

APPENDIX

TEST METHOD USED IN THE PREFLIGHT JET

Test-Facility Characteristics

The tests in the test unit of the preflight jet of the Langley Pilotless Aircraft Research Station at Wallops Island, Va., are made in a free jet issuing from approximately 27-inch-square nozzles at subsonic Mach numbers up to approximately 0.95 and at supersonic Mach numbers of 1.4, 1.6, 1.8, and 2.0. The static pressure of the jet is adjusted to equal the static pressure of the ambient still air and is therefore approximately equal to 2,116 pounds per square foot. The stagnation temperature may be varied between 600° and 1,060° Rankine.

At supersonic speeds, the region upstream of the nozzle exit available for testing is contained within a wedge defined as follows: The base is the nozzle exit, the sides are inclined at the appropriate Mach angle, the vertex edge is vertical, and the ends are the flat top and bottom walls of the nozzle. (The nozzles are two-dimensional.) The region downstream of the nozzle exit available for testing is defined by a pyramid the base of which is the nozzle exit and the sides of which are inclined at the appropriate Mach angle. (See fig. 5.) Because the high-speed photographs are taken from the side of the jet along a line at right angles to the nozzle center line, only the region downstream of the nozzle exit can be used to observe the dynamic behavior of a model; the region inside the nozzle and upstream of the exit may, however, include those parts of the parent aircraft required for proper simulation of the interference flow field.

Photographic Method

The high-speed photographs are made by continuously illuminating the model and exposing the film through narrow radial slits in a rapidly rotating disk placed in front of a camera. Up to 1,000 exposures per second may be taken. The result is a series of images of the model taken at fixed time intervals superimposed on a single 8- by 10-inch photograph. The test setup is shown in figure 3; a typical drop photograph is shown in figure 6.

L

REFERENCES

- 1. Scherberg, Max, and Rhode, R. V.: Mass Distribution and Performance of Free Flight Models. NACA TN 268, 1927.
- 2. Neihouse, Anshal I., and Pepoon, Philip W.: Dynamic Similitude Between a Model and a Full-Scale Body for Model Investigation at Full-Scale Mach Number. NACA TN 2062, 1950.
- 3. Murphy, Glenn: Similitude in Engineering. The Ronald Press Co., 1950, pp. 17-41.

NACA IN 5907

TABLE I.- SUMMARY OF SIMULATION METHODS

The Mach numbers, air properties, static air temperatures, nondimensional radii of gyration in pitch, and the aerodynamic coefficients must be equal for model and prototype. The models must, of course, be geometrically similar to the prototypes.

Light-model method		Modified light-model method		Heavy-model method	
Conditions	Results	Conditions	Results	Conditions	Results
	$\left(\frac{t_X}{L}\right)_M = \left(\frac{t_X}{L}\right)_P$		$\left(\frac{t_X}{L}\right)_M = \left(\frac{t_X}{L}\right)_P$		$\left(\frac{t_X}{\sqrt{L}}\right)_M = \left(\frac{t_X}{\sqrt{L}}\right)_P$
	$(L\ddot{x})_{M} = (L\ddot{x})_{P}$		$(\mathbf{L}\mathbf{\ddot{x}})_{\mathbf{M}} = (\mathbf{L}\mathbf{\ddot{x}})_{\mathbf{P}}$		$(\ddot{x})_{M} = (\ddot{x})_{P}$ $/\dot{x}_{tx} - /\dot{x}_{tx}$
*	$(\dot{x}_{tx})_{M} = (\dot{x}_{tx})_{P}$	(n) (n)	$(\hat{x}_{tx})_{M} = (\hat{x}_{tx})_{p}$		$\left(\frac{\dot{x}_{tx}}{\sqrt{L}}\right)_{M} = \left(\frac{\dot{x}_{tx}}{\sqrt{L}}\right)_{P}$
	$\left(\frac{\mathbf{x}_{tx}}{\mathbf{L}}\right)_{M} = \left(\frac{\mathbf{x}_{tx}}{\mathbf{L}}\right)_{P}$	$\left(\frac{\underline{p}}{\underline{d}}\right)_{\underline{M}} = \left(\frac{\underline{p}}{\underline{d}}\right)_{\underline{p}}$	$\left(\frac{x_{tx}}{L}\right)_{M} = \left(\frac{x_{tx}}{L}\right)_{P}$	(n) (P)	$\left(\frac{x_{tx}}{L}\right)_{M} = \left(\frac{x_{tx}}{L}\right)_{P}$
$\left(\frac{\mathbf{p}}{\mathbf{d}}\right)_{\mathbf{M}} = \left(\frac{\mathbf{p}}{\mathbf{d}}\right)_{\mathbf{P}}$	z and ž _{tx} not implicitly related to L	$(\dot{x}_0)_M = (\dot{x}_0)_P = 0$ $\dot{z}_{0,M} = \dot{z}_{0,P}$	$\left(\mathbf{L}\ddot{\mathbf{z}} \right)_{\mathbf{M}} = \left(\mathbf{L}\ddot{\mathbf{z}} \right)_{\mathbf{P}}$	$\left(\frac{\underline{p}}{dL}\right)_{M} = \left(\frac{\underline{p}}{dL}\right)_{P}$ $\left(\dot{x}_{O}\right)_{M} = \left(\dot{x}_{O}\right)_{P} = 0$	$(\ddot{z})_{M} = (\ddot{z})_{P}$
$(\dot{\mathbf{x}}_0)_{\mathbf{M}} = (\dot{\mathbf{x}}_0)_{\mathbf{P}} = 0$	$\left(\frac{z_{tx}}{L}\right)_{M} = \left(\frac{z_{tx}}{L}\right)_{P}$	(LéO) _M = (LéO) _P	$(\dot{z}_{tx})_{M} = (\dot{z}_{tx})_{P}$	ż _{O,M} (from eq. (30))	$\left(\frac{z_{\pm x}}{\sqrt{L}}\right)_{M} = \left(\frac{z_{\pm x}}{\sqrt{L}}\right)_{P}$
$\dot{z}_{O,M}$ (from eq. (9)) $\left(\dot{L}\dot{\theta}_{O}\right)_{M} = \left(\dot{L}\dot{\theta}_{O}\right)_{P}$ $\alpha_{O,M}$ (from eq. (16))	$\left(L^{2}\overrightarrow{\theta}\right)_{M} = \left(L^{2}\overrightarrow{\theta}\right)_{P}$	$a_{O,M}$ (from eq. (16)) Parent model accelerated upward at rate of $\begin{pmatrix} I_P - 1 \\ I_M \end{pmatrix} g$ starting at $t = 0$	$\left(\frac{z_{tx}}{L}\right)_{M} = \left(\frac{z_{tx}}{L}\right)_{P}$	$\left(\sqrt{L}\dot{\theta}_{0}\right)_{M} = \left(\sqrt{L}\dot{\theta}_{0}\right)_{P}$ $\alpha_{0,M} (\text{from eq. } (36))$	$\begin{pmatrix} \frac{z_{t,x}}{L} \end{pmatrix}_{M} = \begin{pmatrix} \frac{z_{t,x}}{L} \end{pmatrix}_{P}$ $\begin{pmatrix} L\ddot{\theta} \end{pmatrix}_{M} = \begin{pmatrix} L\dot{\theta} \end{pmatrix}_{P}$
	$(L\dot{\theta}_{tx})_{M} = (L\dot{\theta}_{tx})_{P}$		$ \left(L^{2} \dot{\theta} \right)_{M} = \left(L^{2} \dot{\theta} \right)_{P} $ $ \left(L \dot{\theta}_{tx} \right)_{M} = \left(L \dot{\theta}_{tx} \right)_{P} $		$ (\sqrt{L}\hat{\theta}_{tx})_{M} = (\sqrt{L}\hat{\theta}_{tx})_{P} $
O,M	$ \left(\theta_{tx} \right)_{M} = \left(\theta_{tx} \right)_{P} $ $ \left(\alpha_{tx} \right)_{M} = \left(\alpha_{tx} \right)_{P} $		$ \left(\theta_{\text{tx}}\right)_{\text{M}} = \left(\theta_{\text{tx}}\right)_{\text{P}} $		$\left(\theta_{tx}\right)_{M} = \left(\theta_{tx}\right)_{P}$
	$\left(\frac{P}{\overline{L}}\right)_{M} = \left(\frac{P}{\overline{L}}\right)_{P}$		$(\alpha_{tx})_{M} = (\alpha_{tx})_{P}$		$(\alpha_{tx})_{M} = (\alpha_{tx})_{P}$
	$\left(\frac{t_1/2}{L}\right)_{M} = \left(\frac{t_1/2}{L}\right)_{P}$		$\begin{pmatrix} \frac{P}{L} \end{pmatrix}_{M} = \begin{pmatrix} \frac{P}{L} \end{pmatrix}_{P}$ $\begin{pmatrix} \frac{t_{1/2}}{L} \end{pmatrix}_{M} = \begin{pmatrix} \frac{t_{1/2}}{L} \end{pmatrix}_{P}$		$\left(\frac{P}{\sqrt{1}}\right)_{M} = \left(\frac{P}{\sqrt{1}}\right)_{P}$ $\left(t_{1/2}\right)_{M} = \left(t_{1/2}\right)_{P}$

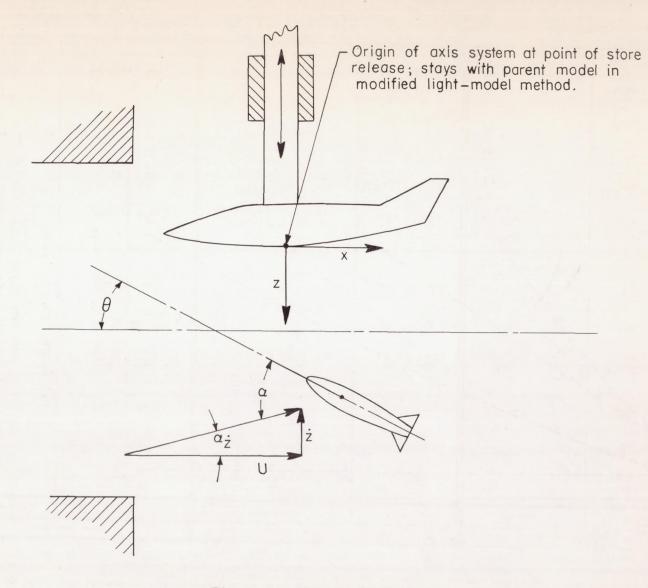
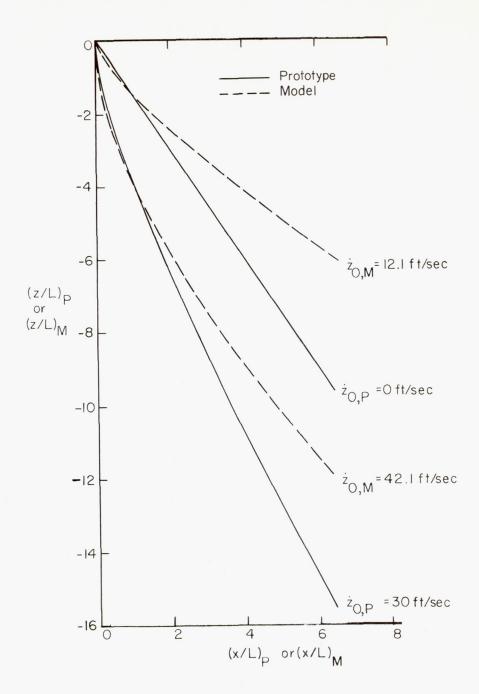
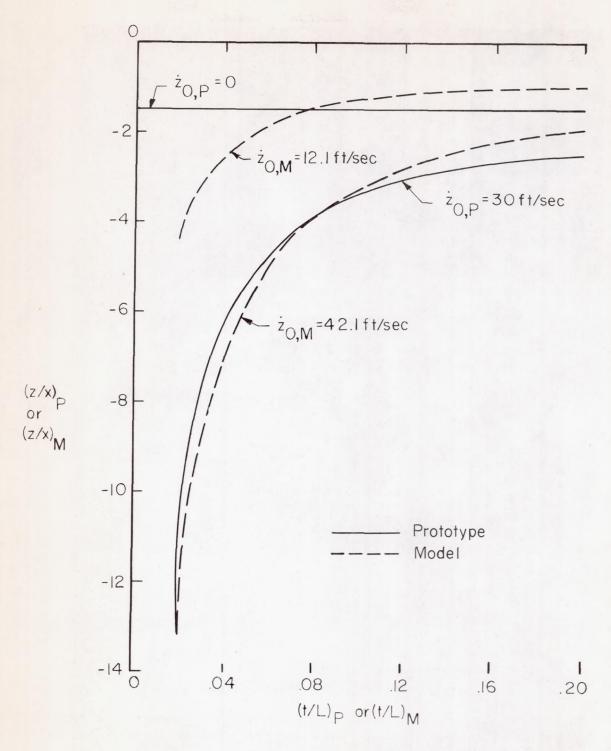


Figure 1.- Coordinate system.



(a) Space trajectories.

Figure 2.- Comparison of model and prototype trajectories for light-model method. Curves calculated assuming uniform flow field; $\dot{z}_{0,M}$ adjusted so that $(z/x)_M = (z/x)_P$ when x/L = 1.0; $K_x p/d = 10$; $K_z p/d = 5$; Lp = 10 feet; LM = 0.5 feet.



(b) Time histories.

Figure 2.- Concluded.

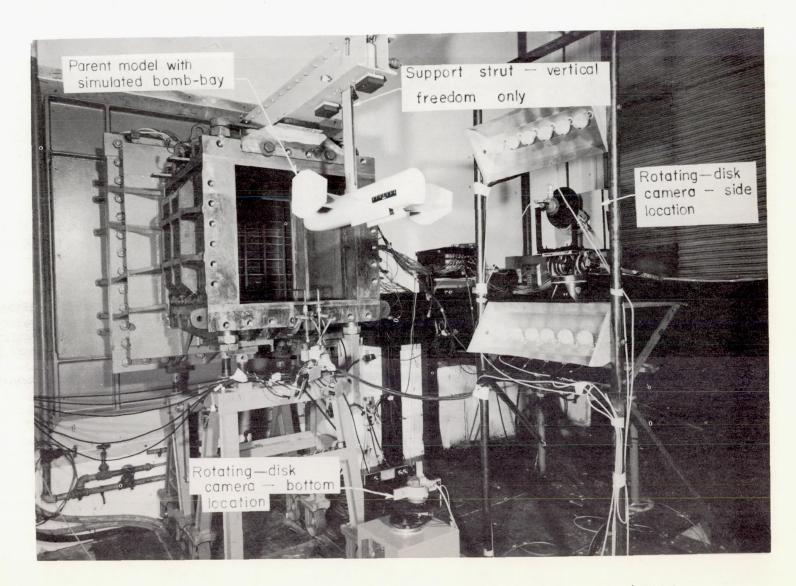
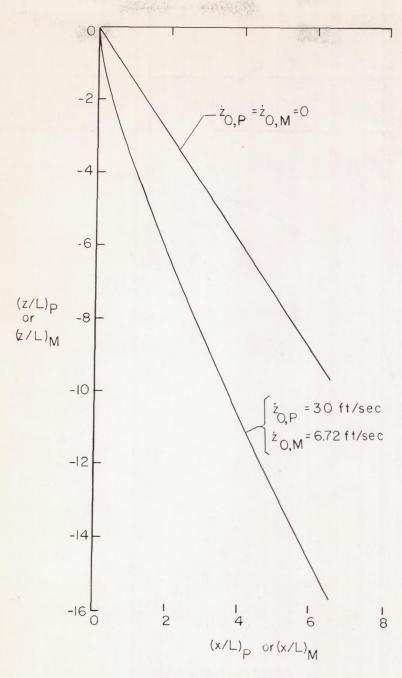
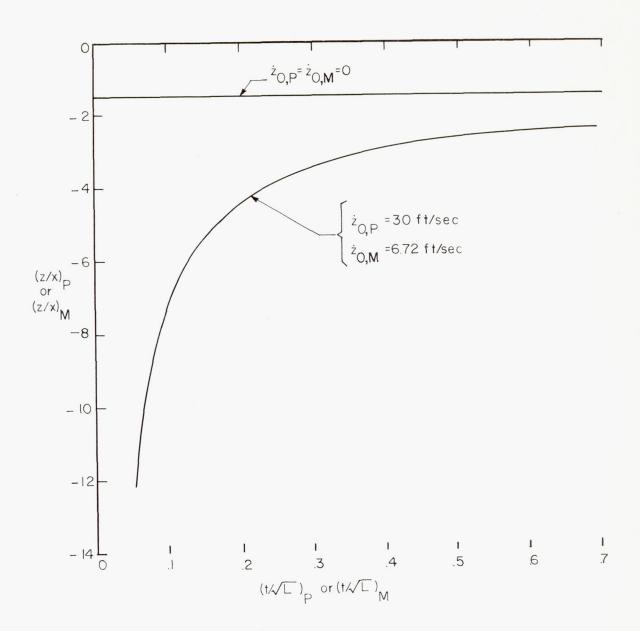


Figure 3.- Typical free-drop setup in the preflight jet. L-94715.1



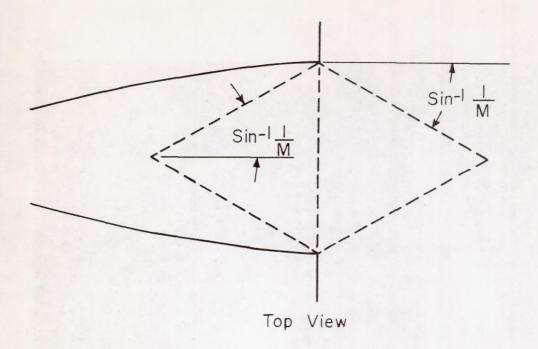
(a) Space trajectories.

Figure 4.- Comparison of model and prototype trajectories for heavy-model method. Curves calculated assuming uniform flow field; $K_{\rm ax}$ = 1.0; $K_{\rm az}$ = 0.5; Lp = 10 feet; $I_{\rm M}$ = 0.5 feet; curves are coincident for values of $\dot{z}_{\rm O}$ specified.



(b) Time histories.

Figure 4.- Concluded.



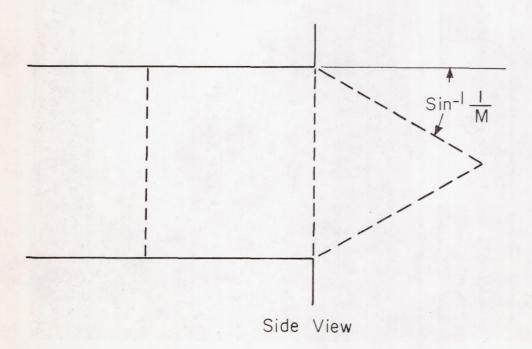
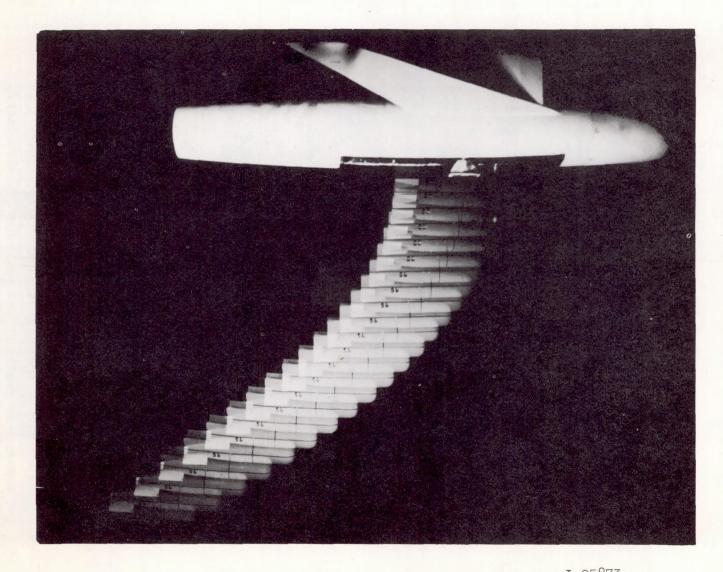


Figure 5.- Region of preflight jet available for drop test.



L-95873
Figure 6.- Typical photographic history of simulated bomb drop.

ACA - Langley Field, Va.